J|A|C|S
ARTICLES
Published on Web 12/08/2006

Methyaluminoxane (MAO) Polymerization Mechanism and Kinetic Model from Ab Initio Molecular Dynamics and Electronic Structure Calculations

Lacramioara Negureanu,[†] Randall W. Hall,*[,†,‡] Leslie G. Butler,[†] and Larry A. Simeral[§]

Contribution from the Department of Chemistry, Louisiana State University, Baton Rouge, Louisiana 70803, and Process Development Center, Albemarle Corporation, Gulf States Road, P.O. Box 341, Baton Rouge, Louisiana 70821

Received June 27, 2006; E-mail: rhall@lsu.edu

Abstract: MAO is the cocatalyst in metallocene catalytic systems, which are widely used in single-site olefin polymerization due to their high stereoselectivity. To date, the structures of the catalytically active compound or compounds in MAO have eluded researchers. Although many structural models have been proposed, none are generally accepted. In this study, aspects of the formation mechanism of MAO are addressed. Molecular dynamics simulations at the MP2 level of theory were carried out for presumed elementary steps in MAO formation via hydrolysis of trimethylaluminum (TMA). Methane production was observed, in agreement with experiment, as well as intermediate species that are consistent with the known structural features of MAO and similar to isolated and structurally characterized aluminoxanes. A $(CH_3)_3$-Al−OH_2 species, which we denote as TMA−OH_2, containing a stable Al−O single bond emerged as the building block molecule. From this species, a hexameric cage was formed and activation barriers for the various reactions were calculated. Three distinct channels were identified for growth beyond the hexameric cage. It was concluded that MAO formation is a step polymerization through a bifunctional monomer, with [(CH_3)Al−O] as the structural unit and a kinetic model was proposed. The structures that emerged were in agreement with the crystallographic evidence for aluminoxanes and support the experimental data regarding the MAO chemical composition.

Introduction

In the past 20 years, polyolefin synthesis has been revolutionized by metallocene single-site catalytic systems in which methylaluminoxane (MAO) is the cocatalyst. These are not only the most highly active catalytic systems for the polymerization of α-olefins, but they produce polymers with high stereoselectivity and narrow molecular weight distributions, giving polymer producers unprecedented control over the synthesis and architecture of their products. Since its discovery, experimental and theoretical studies have been conducted with the goal of understanding, modifying, improving, and extending this catalyst family. MAO is the most active cocatalyst of metallocene catalysts; however, it is also the most difficult to characterize. Despite an intense research effort, the structure of MAO, the mechanism by which the cocatalyst activates the metallocene, and the polymerization mechanism at the active site are not fully understood.

The structure and function of MAO in metallocene single-site catalysts have been the subject of a large number of studies as reflected in recent reviews.[1,2] MAO, a white amorphous powder that is soluble in toluene and other aromatic solvents and highly reactive with air, does not lend itself to a direct spectroscopic characterization.[3] In the past few years, fast computers and parallel computing have allowed theoretical studies of MAO. Many structural models have been proposed by different groups[2,4] but there is not a generally accepted one. ^{27}Al and ^{17}O NMR investigations[5] and crystallographic evidence for other alkylalumoxanes (*tert*-butylalumoxane)[6] have led to a general agreement that MAO is a multicomponent material with three-dimensional cage-like cluster structures, composed of square, hexagonal, and/or octagonal faces, in which four-coordinate aluminum centers are bridged by three-coordinate oxygen atoms. MAO composition is often described in terms of the methyl-to-aluminum ratio. The most commonly reported CH_3/Al ratio is in range of 1.4−1.5;[1,7] values higher than 1.5 and lower than 1.1 have also been reported, and most importantly, the ratio is always greater than 1. However, the most commonly proposed models for the MAO structure[2] have a CH_3/

[†] Louisiana State University.
[‡] Also Department of Physics and Astronomy, Louisiana State University, Baton Rouge, LA 70803.
[§] Albemarle Corp.

(1) Kaminsky, W. *J. Polym. Sci., Part A: Polym. Chem.* **2004**, *42*, 3911.
(2) Zurek, E.; Ziegler, T. *Prog. Polym. Sci.* **2004**, *29*, 107.
(3) Bryant, P. L.; Harwell, C. R.; Mrse, A. A.; Emery, E. F.; Gan, Z.; Caldwell, T.; Reyes, P. A.; Hoyt, D. W.; Simeral, L. S.; Hall, R. W.; Butler, L. G. *J. Am. Chem. Soc.* **2001**, *123*, 12009.
(4) Ystenes, M.; Eilertsen, J. L.; Liu, J. K.; Ott, M.; Rytter, E.; Stovneng, J. A. *J. Polym. Sci., Part A: Polym. Chem.* **2000**, *38*, 3106.
(5) Babushkin, D. E.; Semikolenova, N. V.; Panchenko, V. N.; Sobolev, A. P.; Zakharov, V. A.; Talsi, E. P. *Macromol. Chem. Phys.* **1997**, *198*, 3845.
(6) Harlan, C. J.; Mason, M. R.; Barron, A. R. *Organometallics* **1994**, *13*, 2957.
(7) Sinn, H. *Macromol. Symp.* **1995**, *97*, 27.

10.1021/ja064545q CCC: $33.50

Al ratio of 1:1. This discrepancy has been explained by making a distinction between "classic" or "pure" or TMA-free MAO (CH_3:Al = 1:1) and "real" or TMA-containing MAO, in which free TMA reacts with "pure" MAO to form a compound with the requisite ratio. However, recent in situ FTIR spectroscopy studies found "real" MAO to be structurally stable with no evidence for a chemical reaction between TMA and TMA-"depleted", "real" MAO,[8] calling into question the above classification of "classic", "real", or "pure" MAO.

In this study, ab initio molecular dynamics (MD) simulations and electronic structure calculations are used to propose a mechanism for MAO formation that results in a class of compounds with CH_3/Al ratios greater than 1 and in the range of the experimental values. The proposed mechanism has all the characteristics of a step polymerization through a bifunctional monomer, TMA−OH_2. Although step polymerization allows any two species to react, for organizational simplicity in this work, the monomer was added to a species to generate new and larger structures. Termination of the polymerization is accomplished by reaction with free TMA. In agreement with the multicomponent nature of MAO, several reaction channels are identified.

Computational Details

The NWChem 4.5[9] computational package was used to obtain the forces in gas-phase MD simulations with Moller−Plesset second-order perturbation energy theory[10] (MP2) and the Los Alamos National Laboratory 2-double-ζ (LANL2DZ) basis set[11] model chemistry. MD simulations have been carried out for proposed elementary steps in MAO formation, until a hexameric cage was formed. Ab initio MD simulations of these reaction systems require a long computational time to overcome activation barriers. To reduce this time, we defined Al−O and C−H attractive forces that were present only in the distance region where the activation barrier was presumed to exist. This approach can be thought of as an importance sampling scheme. The attractive forces reduced reaction activation barriers and allowed reactions to occur in a tractable amount of computer time. Defining r_L and r_U as the lower and upper limits of this distance region, respectively, the attractive forces were derived from the following cubic potential energy:

$$V(r) = \frac{3\Delta E}{(r_U - r_L)^2 \beta}\left[(r - r_L)^2 - \frac{2(r - r_L)^3}{3(r_U - r_L)}\right] \quad (1)$$

Here, ΔE is a dimensionless measure of the amount of energy by which the barrier is reduced, and $\beta = (1/k_B T)$. The resulting forces are zero at the boundaries of the defined region, so that a molecule entering or leaving this region would not experience a sudden force. ΔE was varied from 5 to 60 for the various reactions that were studied. The reaction trajectories were used as input to standard ab initio procedures for determining activation barriers and thermodynamic quantities. Initial velocities for the MD simulations were set to zero and rescaled after 20−40 passes to simulate a constant temperature in the range of 300−500 K. We used several different initial geometries in the first MD runs and chose the reactive ones for further analysis.

Minimum energy structures, activation energies and thermodynamic data have been calculated using the B3LYP[12] density functional hybrid, and in some cases the MP2 level of theory in the frozen core approximation, with 6-31g**[13] polarized basis sets, as implemented in Gausssian98[14] and Gaussian03.[15] Zero-point energy corrections to electronic energies were calculated from the vibrational frequencies and used unscaled. Analytical gradient techniques have been used for both minimizations and frequency calculations.

For trimethylaluminum and the trimethylaluminum dimer (TMA_2), MP2 level theory is required for accuracy.[16] However, we found that in electronic structure calculations for alkylalumoxane compounds, the B3LYP and MP2 methods gave similar results, in agreement with previous studies,[2] thus most of our calculations used the B3LYP level of theory. In all the cases, transition states were verified to have the required number of negative eigenvalues. Aside from this local criterion, in all the cases, the intrinsic reaction coordinates calculations (IRC) using Gonzalez-Schlegel method was performed in order to verify the minima connected through the transition state. The IRC is defined as the minimum energy reaction pathway in mass-weighted Cartesian coordinates between the transition state of a reaction and its reactants and products.

MAO synthesis typically occurs in toluene.[17,18] Given the nonpolar nature of the solvent, we expected solvent effects to be negligible, as has been seen previously.[19] Therefore, solvent effects were not included in the calculations. All thermodynamic properties were calculated at 298.15 K and 1 atm pressure.

Results and Discussion

A. MAO Polymerization Mechanism. MAO is usually prepared by the carefully controlled reaction of trimethylaluminum and water, which is the source of oxygen. The reaction is highly exothermic, and at high water concentrations, explosions are possible. Direct hydrolysis preparation methods include the Kaminsky and Haehnsen method in which ice is the source of water and the reaction conditions are quite difficult to control and crystallized water methods in which salt hydrates such as $CuSO_4 \cdot 5H_2O$ or $Al_2(SO_4)_3 \cdot 18H_2O$ are the source of water, allowing more precise control of the amount of water in the reaction system. Non-hydrolytic approaches have been reported,[20] but they have not replaced the hydrolytic process for producing industrial-scale quantities of MAO for use in single-site catalytic systems.

Initiation. Trimethylaluminum is known to dimerize even in gas phase with experimental gas-phase association enthalpy and free Gibbs energy of -20.40 ± 0.34 kcal/mol[21] and -7.6 kcal/mol,[22] respectively. From previous studies, MP2 calculations for TMA dimerization are consistent with the experimental energetics as well as the TMA_2 electron diffraction geometry.[16] The calculated gas-phase reaction path for TMA dimerization using the ab initio MP2 method is shown in Figure 1. As expected, the energetics favor the dimer formation; hence subsequent MD simulations used the TMA dimer as a starting point.

(8) Eilertsen, J. L.; Rytter, E.; Ystenes, M. *Vib. Spectrosc.* **2000**, *24*, 257.
(9) High Performance Computational Chemistry Group. *A Computational Chemistry Package for Parallel Computers*, Version 4.5; Pacific Northwest National Laboratory: Richland, WA, 2003.
(10) Head-Gordon, M.; Pople, J. A.; Frisch, M. J. *Chem. Phys. Lett.* **1988**, *153*, 503.
(11) Hay, P. J.; Wadt, W. R. *J. Chem. Phys.* **1985**, *82*, 299.
(12) Becke, A. D. *J. Chem. Phys.* **1993**, *98*, 5648.
(13) Francl, M. M.; Pietro, W. J.; Hehre, W. J.; Binkley, J. S.; Gordon, M. S.; DeFrees, D. J.; Pople, J. A. *J. Chem. Phys.* **1982**, *77*, 3654.
(14) Frisch, M. J.; et al. *Gaussian 98*, revision A.11.4; Gaussian, Inc.: Pittsburgh, PA, 2002.
(15) Frisch, M. J.; et al. *Gaussian 03*, revision C.02; Gaussian, Inc.: Wallingford, CT, 2004.
(16) Willis, B. G.; Jensen, K. F. *J. Phys. Chem. A* **1998**, *102* 2613.
(17) Nowlin, T. E.; Lo, F. Y.; Shinomoto, R. S.; Shirodkar, P. P. Process and a catalyst for preventing reactor fouling. U.S. Patent 5,332,706, 1994.
(18) Kaminsky, W.; Kulper, K.; Buschermohle, M.; Luker, H. Process for the preparation of polyolefins. U.S. Patent 4,769,510, 1988.
(19) Zurek, E.; Ziegler, T. *Inorg. Chem.* **2001**, *40*, 3279.
(20) Smith, M. G.; Rogers, S. Jonathan *Proceedings of Metallocene Europe '98*; The 5th International Congress in Metallocene Polymers; Germany, 1998.
(21) Henrickson, C. H.; Eyman, D. P. *Inorg. Chem.* **1967**, *6*, 1461.
(22) Smith, M. B. *J. Organomet. Chem.* **1972**, *46*, 31.

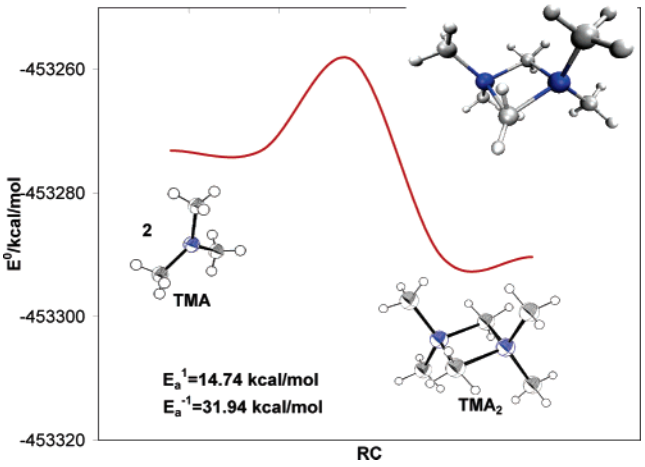

Figure 1. Calculated reaction path for TMA dimerization using the MP2/6-31g** model chemistry. E_a^1 is the activation barrier for the forward reaction, while E_a^{-1} is the activation barrier for the reverse reaction. In the molecular representations, the Al atoms are blue, O atoms are red, C atoms are gray, and H atoms are white.

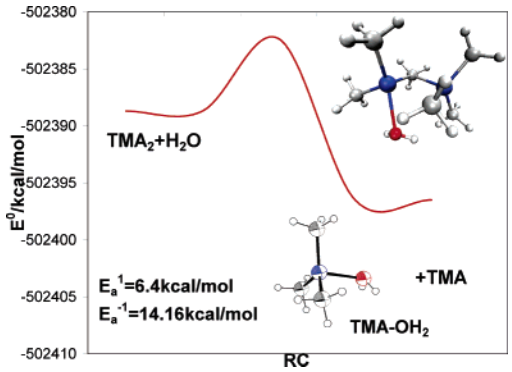

Figure 2. Calculated reaction path for the TMA_2 reaction with water, using the B3LYP/6-31g** model chemistry. All subsequent calculated reaction paths used the B3LYP/6-31g** model chemistry.

An ab initio MD simulation found that the dimer reacts with water to form free TMA and $(CH_3)_3Al-OH_2$, as seen in Figure 2. The activation energy for the forward reaction is less than one-half the activation energy for the reverse reaction. ^{1}H NMR spectroscopic evidence for $TMA-OH_2$ existence in a polar solvent (diethyl ether) was reported by Boleslawski et al.[23] Natural bond orbital analysis[15] of $TMA-OH_2$, at B3LYP/6-31g** level, shows a sigma Al−O sigma bond with more than 95% contribution from the oxygen to the bonding orbital (details in Supporting Information). The length of the Al−O bond in the optimized geometry of $TMA-OH_2$ for both MP2 and B3LYP methods with 6-31g** basis sets is 2.09 Å, in the range of the typical Al−O single bond.[24] With the hypothesis that $TMA-OH_2$ could act as the monomer in the formation of MAO, we performed MD simulations of the reaction between $TMA-OH_2$ and various species that appeared during our investigation (*vida infra*).

Dimer Formation. Ab initio MD simulations indicated that the newly formed $TMA-OH_2$ species may further react with TMA, as shown in Figure 3, forming a four-atom ring that includes a bridging methyl ($M_2^{1'}$, refer to footnote b in Table 1 regarding the terminology used to label the species studied in this work), or react with itself forming a four-membered Al_2O_2 ring ($M_2^{2''}$, Figure 4) as proposed in other initial reaction schemes.[23,25]

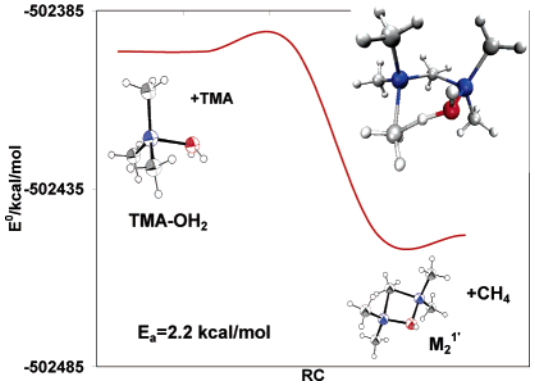

Figure 3. Calculated reaction path for the $TMA-OH_2$/TMA system.

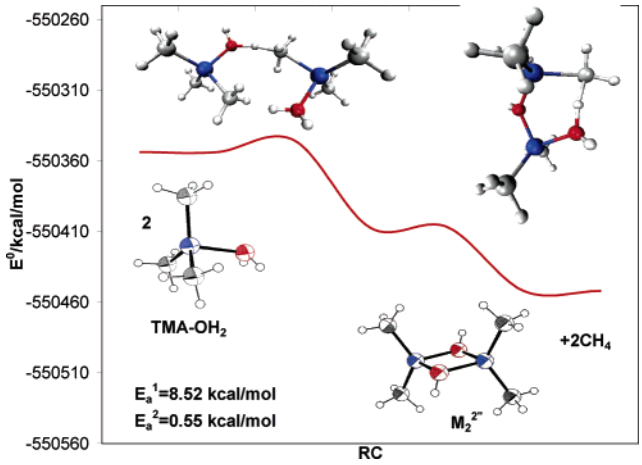

Figure 4. Calculated reaction path for the dimer, $M_2^{2''}$, formation by $TMA-OH_2$ dimerization.

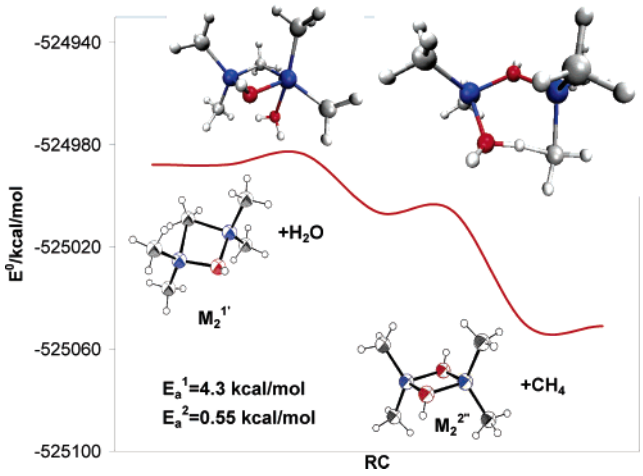

Figure 5. Calculated reaction path for the methyl bridge displacement in $M_2^{1'}$ by water to form $M_2^{2''}$.

Although the activation energy for the first process is lower, thermodynamically $TMA-OH_2$ dimerization is preferred; ΔG for the dimer ($M_2^{2''}$) formation is 57.55 kcal/mol more negative than the ΔG for $M_2^{1'}$ formation (see Table 1). An alternative to the direct dimerization was found via ab initio MD simulations

(23) Boleslawski, M.; Serwatowski, J. *J. Organomet. Chem.* **1983**, *255*, 269.
(24) Zaworotko, M. J.; Rogers, R. D.; Atwood, J. L. *Organometallics* **1982**, *1*, 1179.
(25) Howie, M. S. *Proceedings of Metallocene Europe'98*; The 5th International Congress in Metallocene Polymers; Germany, 1998.

Table 1. Steps in MAO Formation: Initiation, Propagation, Termination[a]

reaction	ΔE°	ΔH	ΔG	theory
$TMA_2 + H_2O \overset{k_2/k_{-2}}{\rightleftharpoons} TMA + TMA{-}OH_2$	−7.79 −1.26	−7.80 −2.23	−13.57 −5.39	B3LYP MP2
$TMA + TMA \overset{k_1/k_{-1}}{\rightleftharpoons} TMA_2$	−8.78 −17.29	−9.53 −16.00 −20.4 ± 0.34	7.07 −4.64 −7.6	B3LYP MP2 exp.[20,21]
$TMA{-}OH_2 + TMA{-}OH_2 \xrightarrow{k_p} M_2^{2''} + 2CH_4$[b]	−98.20	−98.31	−104.51	B3LYP
$M_2^{2''} + TMA{-}OH_2 \xrightarrow{k_p} M_3^{3''} + 2CH_4$	−78.34	−80.35	−82.91	B3LYP
$M_3^{3''} + TMA{-}OH_2 \xrightarrow{k_p} M_4^{4''}{-}1 + 2CH_4$	−83.08	−80.86	−91.00	B3LYP
$M_3^{3''} + TMA{-}OH_2 \xrightarrow{k_p} M_4^{4''}{-}2 + 2CH_4$	−81.20	−79.10	−88.80	B3LYP
$M_4^{4''} + TMA{-}OH_2 \xrightarrow{k_p} M_5^{5''}{-}1 + 2CH_4$	−74.60	−74.45	−81.08	B3LYP
$M_4^{4''} + TMA{-}OH_2 \xrightarrow{k_p} M_5^{5''}{-}2 + 2CH_4$	−78.42	−78.24	−84.88	B3LYP
$M_2^{2''} + M_3^{3''} \xrightarrow{k_p} M_5^{5''}{-}3 + 2CH_4$	−76.89	−74.42	−84.58	B3LYP
$M_5^{5''}{-}2 + TMA{-}OH_2 \xrightarrow{k_p} M_6^{6''}{-}1 + 2CH_4$	−78.75	−79.85	−82.17	B3LYP
$M_3^{3''} + M_3^{3''} \xrightarrow{k_p} M_6^{6''}{-}2 + 2CH_4$	−91.96	−87.56	−100.10	B3LYP
$M_2^{2''} + M_4^{4''}{-}2 \xrightarrow{k_p} M_6^{6''}{-}2 + 2CH_4$	−89.25	−88.80	−94.22	B3LYP
$M_5^{5''}{-}1 + TMA{-}OH_2 \xrightarrow{k_p} M_6^{6} + 4CH_4$	−151.86	−151.77	−175.66	B3LYP
$M_6^{6''}{-}2 \rightarrow M_6^{6} + 2CH_4$	−40.92	−40.87	−60.20	B3LYP
$M_6^{6}{-}1 + TMA{-}OH_2 \xrightarrow{k_p} M_7^{7'}{-}1 + CH_4$[c]	−68.44	−68.76	−63.14	B3LYP
$M_6^{6} + TMA{-}OH_2 \xrightarrow{k_p} M_7^{7'}{-}2 + CH_4$	−60.25	−60.14	−56.29	B3LYP
$M_6^{6} + TMA{-}OH_2 \xrightarrow{k_p} M_7^{7'}{-}3 + CH_4$	−36.75	−34.40	−34.23	B3LYP
$M_7^{7'} + TMA{-}OH_2 \xrightarrow{k_p} M_8^{8'}{-}11 + 2CH_4$	−98.16	−97.93	−104.16	B3LYP
$M_6^{6} + M_2^{2''} \xrightarrow{k_p} M_8^{8'}{-}11 + CH_4$	−68.42	−68.38	−62.78	B3LYP
$M_7^{7'} + TMA{-}OH_2 \xrightarrow{k_p} M_8^{8'}{-}12 + 2CH_4$	−84.05	−83.65	−90.85	B3LYP
$M_8^{8'}{-}11 \rightarrow M_8^{8} + CH_4$	−24.50	−24.33	−34.38	B3LYP
$M_8^{8'}{-}11 + TMA{-}OH_2 \xrightarrow{k_p} M_9^{9'}{-}11 + 2CH_4$	−89.92	−90.06	−94.67	B3LYP
$M_8^{8} + TMA{-}OH_2 \xrightarrow{k_p} M_9^{9'}{-}11 + CH_4$	−65.42	−65.73	−60.28	B3LYP
$TMA{-}OH_2 \rightarrow (CH_3)_2AlOH + CH_4$	−22.48 −20.48	−22.80 −15.09	−31.76 −31.65	B3LYP MP2
$(CH_3)_2AlOH + (CH_3)_2AlOH \rightarrow M_2^{2''}$	−52.22 −60.47	−52.70 −50.36	−40.99 −44.56	B3LYP MP2
$TMA{-}OH_2 + TMA \xrightarrow{k_t} M_2^{1'} + CH_4$	−51.54 −57.14	−51.88 −56.54	−46.96 −54.05	B3LYP MP2
$M_2^{1'} + H_2O \rightarrow M_2^{2'} + CH_4$	−63.24 −62.76	−63.76 −63.18	−64.06 −63.84	B3LYP MP2
$M_2^{1'} + TMA \xrightarrow{k_t} M_3^{1} + CH_4$	−41.00	−40.46	−39.36	B3LYP
$M_3^{3'} + TMA \xrightarrow{k_t} M_4^{3'} + CH_4$	−39.96	−38.03	−38.42	B3LYP
$M_7^{7'}{-}1 + TMA \xrightarrow{k_t} M_8^{7}{-}11 + CH_4$	−40.03	−40.11	−34.89	B3LYP
$M_7^{7'}{-}1 + TMA \xrightarrow{k_t} M_8^{7}{-}12 + CH_4$	−38.21	−37.96	−34.25	B3LYP
$M_7^{7'}{-}1 + TMA \xrightarrow{k_t} M_8^{7}{-}13 + CH_4$	−37.86	−37.80	−35.57	B3LYP
$M_8^{8'}{-}11 + TMA \xrightarrow{k_t} M_9^{8}{-}11 + CH_4$	−34.60	−35.05	−28.46	B3LYP
$M_8^{8} + TMA \xrightarrow{k_t} M_9^{8}{-}11$	−10.08	−10.72	5.92	B3LYP

[a] Calculated thermodynamic data in kcal/mol at 298.15 K and 1 atm pressure. The basis set for all calculations was 6-31g**. [b] In $M_i^{j'','''}$, or, $'''$ *i* stands for the total number of Al atoms, *j* for the total number of O atoms, and $'$, $''$, and $'''$ denotes one, two, or three −OH functional groups, respectively. For example, $M_3^{3''}$ is a species that contains three Al atoms, and three O atoms, of which two O atoms are part of hydroxyl functional groups. In addition, to distinguish different isomers a dash followed by a number (1, 2, or 3) is added to the previously described notation scheme. $M_4^{4''}{-}1$ denotes the cage-like tetramer whereas $M_4^{4''}{-}2$ denotes the ladder-like tetramer. $M_5^{5''}{-}1$ denotes the cage-like pentamer, $M_5^{5''}{-}2$ denotes the ladder-like pentamer, and $M_5^{5}{-}3$ denotes the pentamer with geometry analogous to isolated *tert*-butyl pentameric hydroxide. $M_6^{6''}{-}1$ denotes the ladder-like hexamer and $M_6^{6''}{-}2$ denotes the hexamer with geometry analogous to the Harlan et al. characterized hexameric hydroxide. [c] Beyond the hexameric cage, the formation of $M_7^{7'}{-}1$, $M_7^{7'}{-}2$, and $M_7^{7'}{-}3$ is a bifurcation point and in order to denote the isomeric species that result from different growth and termination motifs, a second number is added to the notation scheme described in footnote b. $M_8^{7}{-}11$ denotes termination motif 1 from the reaction of TMA with $M_7^{7'}{-}1$. Similarly, $M_8^{7}{-}12$ denotes termination motif 2 from the reaction of TMA with $M_7^{7'}{-}1$.

of the addition of a water molecule to the $M_2^{1'}$ species, as shown in Figure 5.

An analogous dimeric hydroxide, $[(^t\mathrm{Bu})_2\mathrm{Al}\ (\mu{-}\mathrm{OH})]_2$, has been isolated by Barron and co-workers[6] by hydrolysis of Al(^{t}Bu)$_3$ in toluene using a hydrated salt, $Al_2(SO_4)_3{\cdot}14H_2O$, or by the addition of water to a refluxing toluene solution of Al(^{t}Bu)$_3$. The same authors consider this dimeric hydroxide remarkably stable to thermolysis and show that it converts

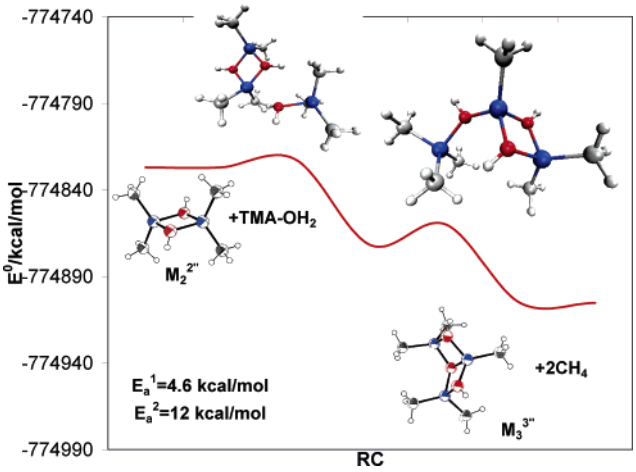

Figure 6. Calculated reaction path for the trimer, $M_3^{3''}$, formation from the dimer.

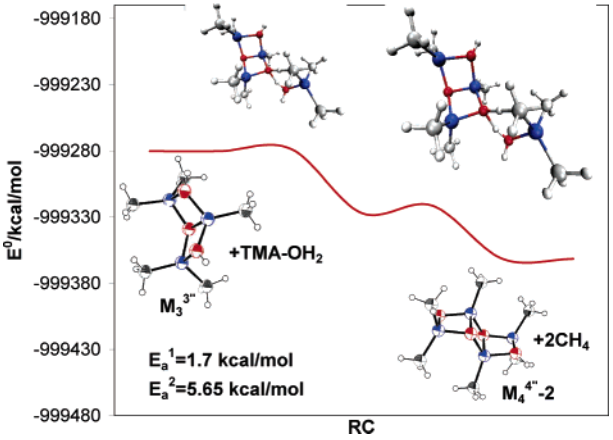

Figure 7. Calculated reaction path for the ladder-like tetramer (three fused Al_2O_2 four-membered rings), $M_4^{4''}-2$, formation from the trimer.

slowly to a mixture of aluminoxane species, $[(^t\mathrm{Bu})_2\mathrm{Al}\ (\mu_3\text{-}\mathrm{O})]_n$, $n = 6-12$.

On the other hand, it has been suggested[23] that $\mathrm{TMA-OH_2}$ could undergo intramolecular methane elimination forming the dimethylaluminum hydroxide, $(\mathrm{CH_3})_2\mathrm{AlOH}$. However, thermodynamically $\mathrm{TMA-OH_2}$ dimerization ($\Delta G = -104.51$ kcal/mol, Table 1) is preferred over the intramolecular elimination ($\Delta G = -31.76$ kcal/mol). In addition, the same authors suggest that in the next step, the dimethylaluminum hydroxide forms what they called a stable autoassociate, which is just the dimeric hydroxide, $M_2^{2''}$, in the proposed mechanism. We find this association is an exoergic process ($\Delta G = -40.99$ kcal/mol, Table 1).

Trimer and Tetramers. Ab initio MD simulation of the reaction between the monomer and the dimer formed a trimer (Figure 6) and a similar simulation of the reaction between the monomer and the trimer yielded a tetramer (Figure 7). These reactions have all the characteristics of a step polymerization through the bifunctional monomer ($\mathrm{TMA-OH_2}$). It is clear that any two species can be coupled, a characteristic of step-polymerization. For simplicity, we investigated the formation of the tetramer via the reaction of the monomer and the trimer; we recognize that the reaction of two dimers to form the tetramer can occur and may have a rate that competes with the monomer/trimer reaction rate.

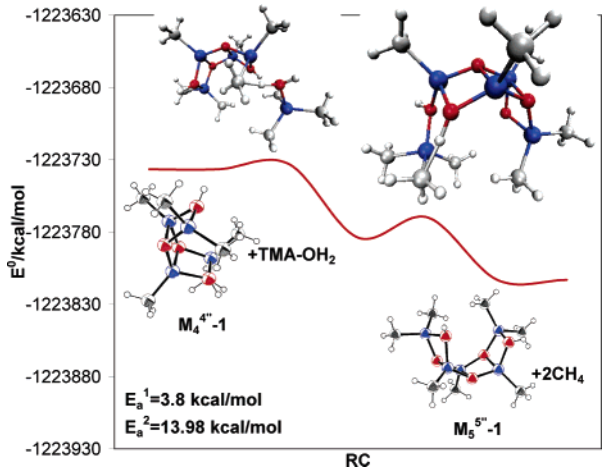

Figure 8. Calculated reaction path for the cage-like pentamer, $M_5^{5''}-1$, formation from the cage-tetramer, $M_4^{4''}-1$.

Polymers synthesized by step-polymerization often have lower average molecular weights and higher dispersity in molecular weight distribution than the polymers synthesized by chain-polymerization. MAO (or polymethylaluminoxane as it is sometimes called[20]) is considered a mixture of oligomers with a broad molecular weight distribution,[17] and 30 hours of reaction time is needed to isolate 19.7 g of methylaluminoxane from 1 mole of water and 0.52 mole trimethylaluminum.[18]

In Figure 6, the growth of the dimer to trimer, two fused four-membered Al_2O_2 rings, is presented. For each monomer added, two methanes are eliminated, and the overall activation energy slightly increases in the dimer to trimer growing process. Reducing the ring strain by breaking Al−O bonds in the trimer structure was considered, and the formation of a ring-opened hexagonal structure by breaking the square-square Al−O bond is not preferred; for such a process $\Delta E° = 23.25$ kcal/mol and $\Delta G = 21.50$ kcal/mol using the B3LYP/6-31g** model chemistry.

The tetramer formation from the trimer is a bifurcation point, as two species were found depending on the initial geometries of the reactants in the ab initio MD simulations, either a ladder-like structure ($M_4^{4''}-2$, Figure 7) or a cage-like structure ($M_4^{4''}-1$, see the reactant in Figure 8). The cage-like structure is 2.2 kcal/mol more stable than the ladder-like structure (Table 1).

Formation of Pentamers, Hexamers, and a Hexameric Cage. Ab initio simulation of the reaction of the monomer with the cage- or ladder-like tetramer generated a cage-($M_5^{5''}-1$, Figure 8) or ladder-($M_5^{5''}-1$, Figure 9) like pentamer. The reaction of the dimer−trimer coupling to form a pentamer was investigated using standard ab initio methods, resulting in a third isomer, $M_5^{5''}-3$ (Figure 10). The molecular structure of $M_5^{5''}-3$ is analogous to the isolated pentameric aluminoxane,[6] and is 17.39 kcal/mol lower in energy than the cage-like pentamer and 15.46 kcal/mol lower in energy than the ladder-like structure. Ab initio MD simulation of the reactions of ladder-like and cage-like pentamer structures with a monomer resulted in a ladder-like structure, $M_6^{6''}-1$ (Figure 11), and an hexameric cage, $[(\mathrm{CH_3})\mathrm{AlO}]_6$ (M_6^6), respectively. $|\Delta G|$ for formation of the cage is relatively large, presumably due to the elimination of four methane molecules (Table 1).

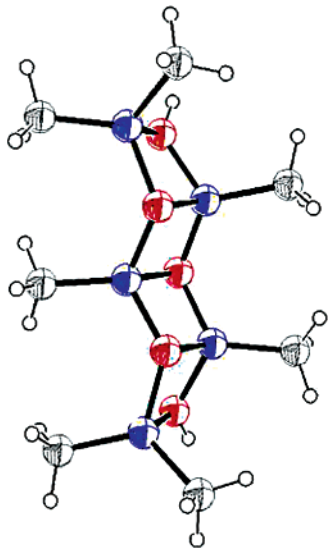

Figure 9. Structure $M_5^{5''}-2$.

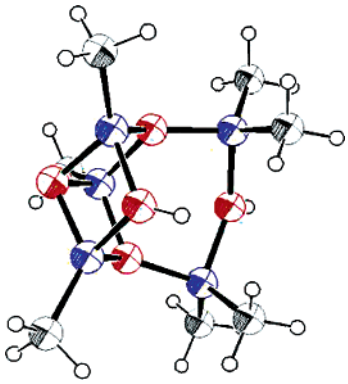

Figure 10. Structure $M_5^{5''}-3$.

An analogous well-known cage for *tert*-butylaluminoxane has been isolated and structurally characterized.[6] In the same study, a hexameric hydroxide structure containing an Al_3O_3 ladder core, present in the trimer (Figure 6) and the cage- and ladder-like pentamers (Figures 8 and 9) in our mechanism, has been isolated and was considered the direct precursor to the isolated hexameric aluminoxane cage. The present mechanism can explain the formation of the isolated hexameric hydroxide structure, analogous to the above $M_6^{6''}-2$ structure (Figure 12), either by reaction of two trimers ($M_3^{3''}$) or by a dimer ($M_2^{2''}$) ladder-like tetramer ($M_4^{4''}-2$) coupling.

Although reactions between monomer and *n*-mers have been simulated to investigate the growth processes, it is clear from the bifunctional nature of the various species that beyond the trimer, there are multiple routes for MAO growth to proceed (for instance, the pentamers could be formed via dimer−trimer growth). Thus, it is possible that the monomer concentration may be already low at this step of the reaction, which is not uncommon because step polymerizations are characterized by the disappearance of the monomer very early in the reaction. Typically, less than 1% of the original monomer remains in the system at the reaction point where the average polymer chain contains ∼10 monomer units (ref 26, page 42). We also note that the cage-like $M_6^{6''}-2$ hexameric hydroxide is much more stable (30.27 kcal/mol) than the ladder-like hexamer ($M_6^{6''}-1$), suggesting that the presence of ladder-like structures after the cage is very unlikely.

(26) Odian, G. *Principles of Polymerization*, 3rd ed.; John Wiley and Sons: New York, 1991.

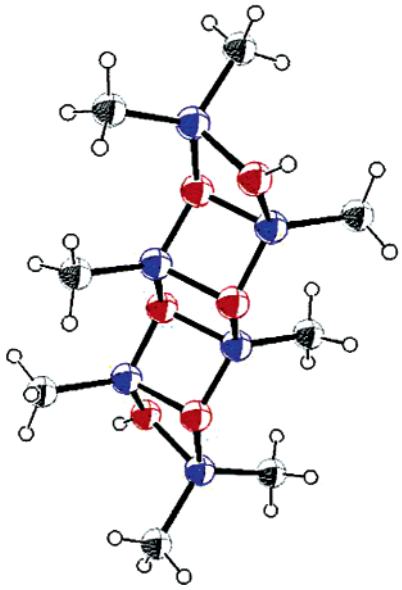

Figure 11. Structure $M_6^{6''}-1$.

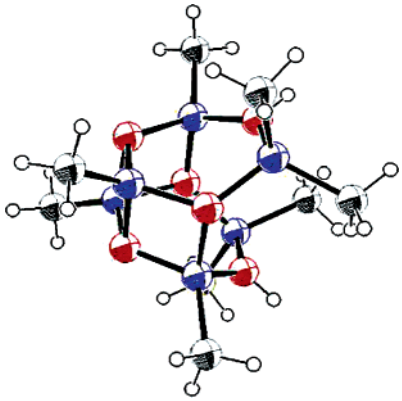

Figure 12. Structure $M_6^{6''}-2$.

Beyond the Hexameric Cage. The reactions of the monomer with the hexameric cage and larger structures were investigated assuming that growth proceeds by the reaction of an −OH group with an $-Al(CH_3)_2$ group to eliminate methane. The insertion of the monomer at the cage can be done in three different ways: breaking a square-square Al−O bond serving as an edge of two four-membered rings, forming $M_7^{7'}-1$ (Figure 13), an axial approach by breaking a square-hexagonal Al−O bond serving as the edge of a four-membered and a six-membered ring, forming structure $M_7^{7'}-1$ (Figure 14), or by reaction of an $-Al(CH_3)$ group from the cage with an −OH group from the monomer forming the $M_7^{7'}-3$ structure (Figure 15). The ΔG for forming compound $M_7^{7'}-1$ from the cage is 6.85 kcal/mol more exoergic than in the case of $M_7^{7'}-2$ and 28.91 kcal/mol than in the case of $M_7^{7'}-3$ formation.

Extensions to the hexameric cage were considered via addition of the monomer to $M_7^{7'}-1$, which can be done in two ways. One way is by breaking another Al−O bond in the cage, forming a new four-membered Al_2O_2 ring, as in $M_8^{8'}-11$ (Figure 16; for the description of the terminology used to designate the species resulting from different growth and

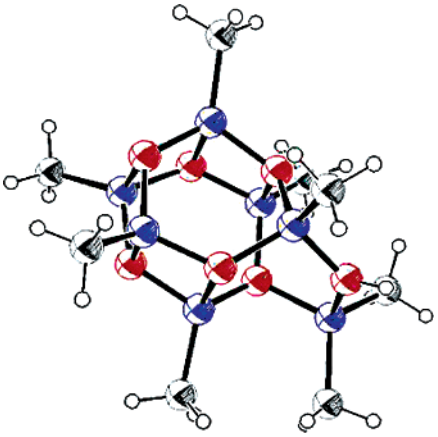

Figure 13. Structure $M_7^{7'}-1$.

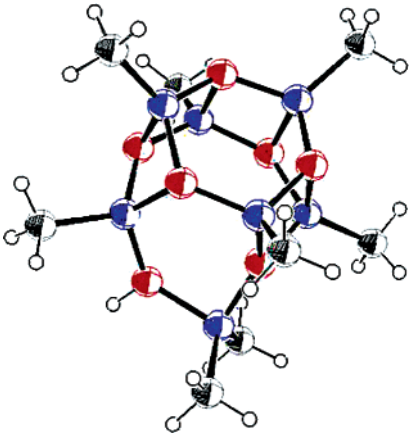

Figure 14. Structure $M_7^{7'}-2$.

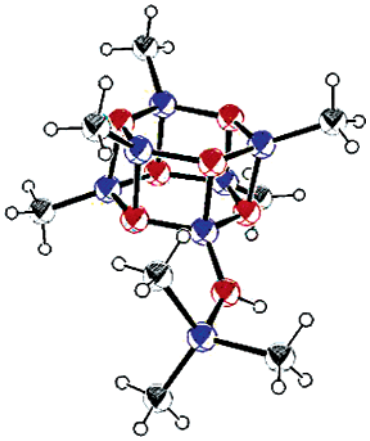

Figure 15. Structure $M_7^{7'}-3$.

termination patterns after the hexameric cage, please refer footnote c in Table 1). In Figure 17, the $M_8^{8'}-12$ structure, a four-membered Al_2O_2 ring is formed outside the cage, though this option is thermodynamically less favorable; ΔG for formation of $M_8^{8'}-12$ from $M_7^{7'}-1$ is 13.31 kcal/mol less exoergic than in the case of formation of $M_8^{8'}-11$ (Table 1). The growth from the cage using the $M_8^{8'}-11$ motif is possible at two identical sites, while the monomer insertion as in $M_8^{8'}-12$ allows a tridirectional growth.

In keeping with the notion that MAO formation is the result of step-polymerization, we note that $M_8^{8'}-11$ can be formed by the reaction of the M_6^6 cage and the $M_2^{2''}$ dimer, with elimination of a methane molecule ($\Delta G = -62.78$ kcal/mol, Table 1). While it is possible for $M_8^{8'}-11$ to undergo intramolecular methane elimination forming structure M_8^8 (Figure 18), the further reaction of $M_8^{8'}-11$ to form $M_9^{9'}-11$ (Figure 19) is favored ($\Delta G = -34.38$ kcal/mol of the latter process as compared to $\Delta G = -94.67$ kcal/mol of the former in Table 1). A structure analogous to M_8^8 has been synthesized in the case of *tert*-butylaluminoxane as the minor product by the reaction of $[(^t\text{Bu})_2\text{Ga}(\mu\text{-OH})]_3$ with $\text{Al}(^t\text{Bu})_3$[6]. M_8^8 could also react with the monomer forming $M_9^{9'}-11$ and releasing a methane molecule ($\Delta G = -60.28$ kcal/mol, Table 1).

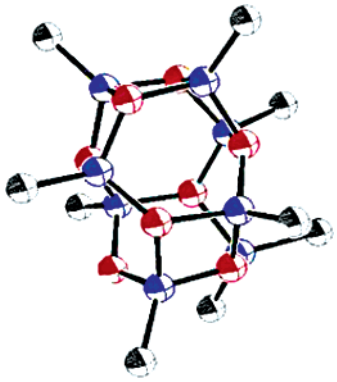

Figure 16. Structure $M_8^{8'}-11$.

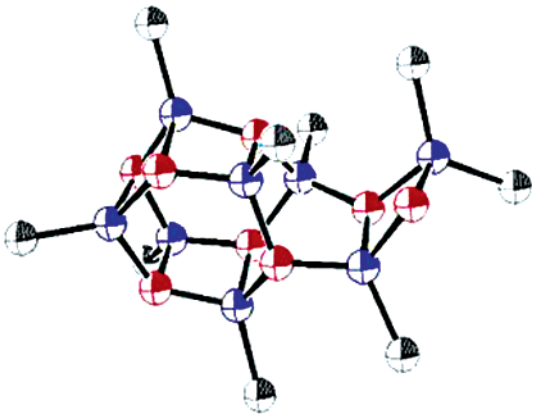

Figure 17. Structure $M_8^{8'}-12$.

This suggests that in the case of *tert*-butylaluminoxane, steric or other considerations may lead to intramolecular methane elimination resulting closed cages whose formation is not favored in methylaluminoxanes. Models similar to M_8^8 closed-cage species have been proposed for MAO,[6] but as shown above, their formation is not a favored reaction route, and they cannot explain MAO chemical composition.

Termination. As mentioned above, studies of TMA hydrolysis[23] show spectroscopic evidence for species with one or more −OH functional groups, similar to the isolated *tert*-butylaluminoxane hydroxides;[6] however, very few if any −OH functional groups are present in the final MAO structure.[27]

Considering the initiation scheme (Table 1), it is likely that the termination of MAO polymerization occurs when TMA, present in the system from the initiation process and TMA_2 dissociation, reacts with −OH functional releasing methane, and any excess TMA is the experimentally observed as residual TMA and TMA_2 in MAO solutions.

(27) Imhoff, D. W.; Simeral, L. S.; Sangokoya, S. A.; Peel, J. H. *Organometallics* **1998**, *17*, 1941.

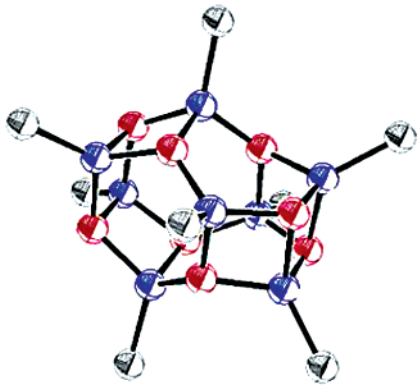

Figure 18. Structure M_8^8.

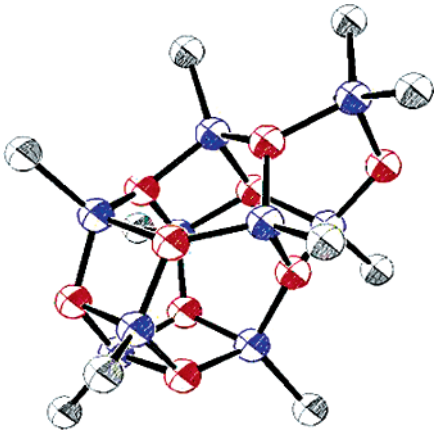

Figure 19. Structure $M_9^{9'}-11$.

Ab initio molecular dynamics simulations of representative termination reactions, Figures 20 and 21, show it is possible for TMA to react with the hydroxyl group(s) of a growing species. The resulting species are not only similar to some of the isolated *tert*-butyl aluminoxanes ($M_4^{3'}$ [6] and M_4^2 [28]), but also they introduce three-coordinate aluminum centers, which have been suggested by NMR studies[3] as possibly present in MAO, and for larger species after the cage the structural motif of bridging methyl groups, that has proven essential for MAO cocatalytic activity.[4]

Activation barriers have been calculated for termination reactions of some of the small species. These barriers are low, less than 1 kcal/mol (Table 1), suggesting that terminated species may be formed before the cage. This may help account for the very broad reported molecular weight distribution in MAO, a 700−3000 g/mol range.[29,30] Interestingly enough, as mentioned above, species similar to $M_4^{3'}$ (Figure 21) have been isolated for *tert*-butylaluminoxane,[6] supporting the proposed MAO formation mechanism.

The termination reaction for species larger than the hexameric cage was investigated by reaction of TMA with $M_7^{7'}-1$. We found the termination can be done in three different ways, M_8^7-11, M_8^7-12, and M_8^7-13 (Figures 22, 23, and 24, respectively). The termination by reaction of an −OH functional with TMA in the M_8^7-11 case involves the breaking of an adjacent square-square Al−O bond at the cage with the formation of a four-membered Al_2O_2 ring and of a six-membered ring through a bridging methyl within the new cage. A four-membered ring containing a bridging methyl is formed outside the cage in the M_8^7-12 case, while in M_8^7-13, the bridging methyl structural motif is missing. In all the cases a methane molecule is eliminated.

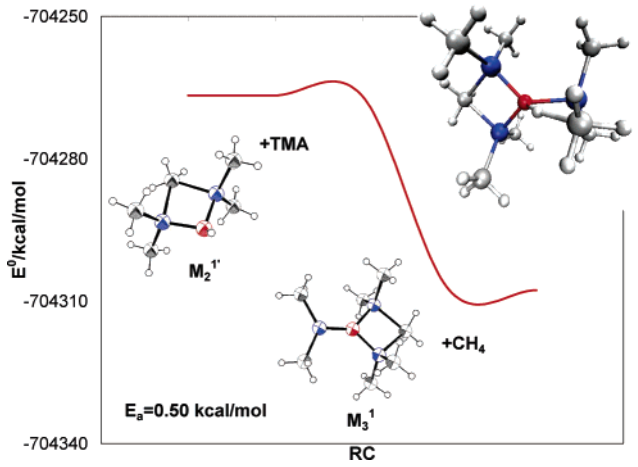

Figure 20. Calculated path for the reaction of TMA and $M_2^{1'}$ to form M_3^1.

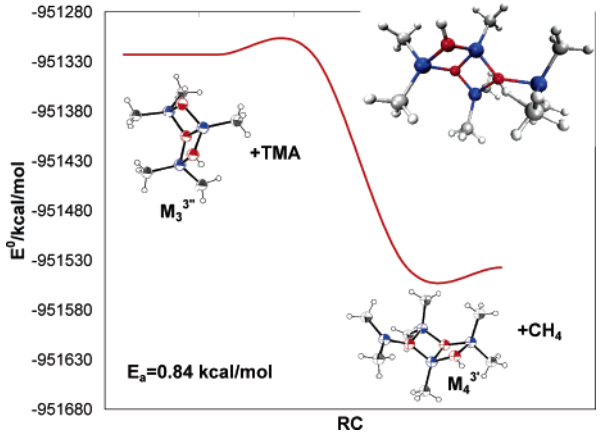

Figure 21. Calculated path for the formation of $M_4^{3'}$ by the partial termination of the trimer by TMA.

Another possible termination after the hexameric cage formation is the insertion of TMA by breaking a square-square Al−O bond, which is known to be more strained than a square-hexagonal bond,[19] in closed-cage structures such as M_8^8, M_9^9, or M_{12}^{12}. In this fashion, the M_9^8-11 structure (Figure 25) is formed by reaction of M_8^8 with TMA, but this reaction route is not energetically favored ($\Delta E^\circ = -10.08$ kcal/mol).

B. The Kinetic Model for MAO Polymerization Mechanism. Evidence from ab initio MD simulations, electronic structure calculations, and experimental structural information for the few alkylaluminoxane species isolated (*tert*-butylaluminoxanes) suggests MAO formation is a step polymerization through a bifunctional monomer, TMA−OH_2. The majority of the growth processes are characterized by the elimination of two methane molecules, whereas the termination involves the elimination of a single methane. Our calculations comparing the growth and termination steps for small clusters (e.g., $M_3^{3''}$) show smaller activation energies for the termination steps but more exoergic reactions for the propagation steps, presumably

(28) Mason, M. R.; Smith, J. M.; Simon, G. B.; Barron, A. R. *J. Am. Chem. Soc.* **1993**, *115*, 4971.
(29) Imhoff, D. W.; Simeral, L. S.; Blevins, D. R.; Beard, W. R. *Olefin Polymerization: Emerging Frontiers*; ACS Symposium Series 749, 2000.
(30) Hansen, E. W.; Blom, R.; Kvernberg, P. O. *Macromol. Chem. Phys.* **2001**, *202*, 2880.

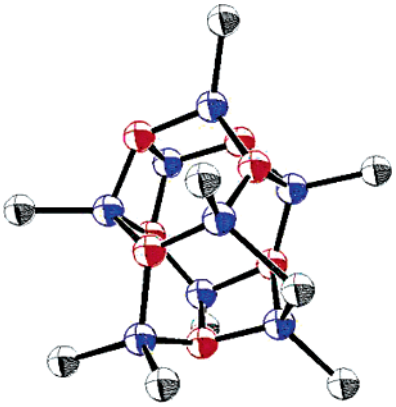

Figure 22. Structure M_8^7-11.

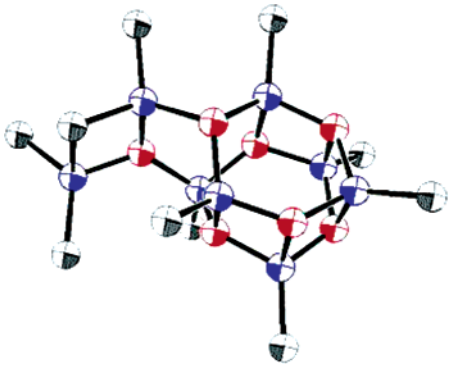

Figure 23. Structure M_8^7-12.

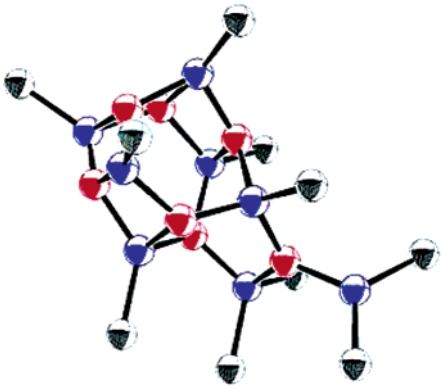

Figure 24. Structure M_8^7-13.

related to the number of methane molecules that are produced. We now formulate the growth process in terms of a step-polymerization kinetic model in which, as commonly done, we assume the concept of equal reactivity of functional groups,[26,31] here $-OH$ and $-Al(CH_3)_2$.

Initiation. The initiation process, corresponding to TMA$-OH_2$ formation, is described by the following two of reactions:

$$TMA + TMA \underset{k_{-1}}{\overset{k_1}{\rightleftharpoons}} TMA_2 \qquad (2)$$

$$TMA_2 + H_2O \underset{k_{-2}}{\overset{k_2}{\rightleftharpoons}} TMA + TMA{-}OH_2 \qquad (3)$$

Propagation. Once the polymerization starts, any two species can react with each other and the process proceeds by a

(31) Flory, P. J. *Principles of Polymer Chemistry*, 1st ed.; Cornell University Press: New York, 1953.

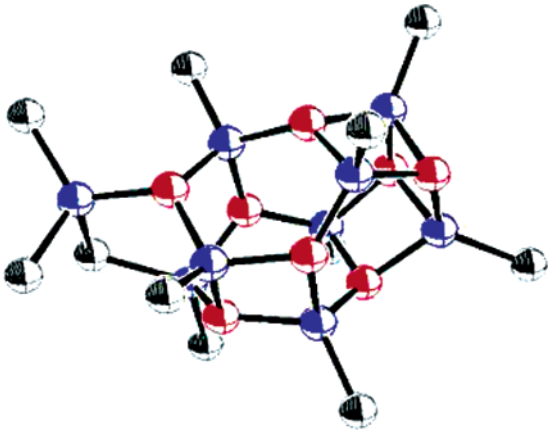

Figure 25. Structure M_9^8-11.

relatively slow increase of the polymer weight, a step polymerization characteristic. The rate constant for growth is denoted by k_p and for simplicity we do not distinguish between most isomers with the same number of $-OH$ groups (e.g., the pentamers). Representative reactions in the propagation are then

$$TMA{-}OH_2 + TMA{-}OH_2 \xrightarrow{k_p} M_2^{2''} + 2CH_4 \qquad (4)$$

$$M_2^{2''} + TMA{-}OH_2 \xrightarrow{k_p} M_3^{3''} + 2CH_4 \qquad (5)$$

$$M_3^{3''} + TMA{-}OH_2 \xrightarrow{k_p} M_4^{4''} + 2CH_4 \qquad (6)$$

$$M_2^{2''} + M_2^{2''} \xrightarrow{k_p} M_4^{4''} + 2CH_4 \qquad (7)$$

$$M_4^{4''} + TMA{-}OH_2 \xrightarrow{k_p} M_5^{5''} + 2CH_4 \qquad (8)$$

$$M_3^{3''} + M_2^{2''} \xrightarrow{k_p} M_5^{5''} + 2CH_4 \qquad (9)$$

$$M_5^{5''} + TMA{-}OH_2 \xrightarrow{k_p} M_6^{6''} + 2CH_4 \qquad (10)$$

$$M_5^{5''} + TMA{-}OH_2 \xrightarrow{k_p} M_6^{6} + 4CH_4 \qquad (11)$$

$$M_7^{7'}{-}1 + TMA{-}OH_2 \xrightarrow{k_p} M_8^{8'}{-}11 + 2CH_4 \qquad (12)$$

$$M_7^{7'}{-}1 + TMA{-}OH_2 \xrightarrow{k_p} M_8^{8'}{-}12 + 2CH_4 \qquad (13)$$

M_6^6 is the hexameric cage and $M_6^{6''}$ is the ladder-like hexamer. After the cage, a bidirectional growth is seen, as in eq 12 for one direction, when the general formula of the generated *n*-mers is HO$-[(CH_3)Al-O]_n-$OH, and a tridirectional growth as in eq 13 when the general formula of the growing species is $[(CH_3)Al-O]_n-(OH)_3$, where *n* is the degree of polymerization.

Termination. It is generally accepted that MAO is a multicomponent material. As discussed above, the termination process is done by reaction of TMA or already partially terminated species with $-OH$ functional at the growing *n*-mers. The final MAO structures have the following general formulas: (i) $(CH_3)_3Al-[(CH_3)Al-O]_n-Al(CH_3)_3$ with $n = 8, 10, 12, 14, \ldots$ for bidirectional growth, (ii) $[(CH_3)Al-O]_n-3Al(CH_3)_3$ with $n = 9, 12, 15, 18, \ldots$ for tridirectional growth, and (iii) $[(CH_3)Al-O]_n-(n-6)Al(CH_3)_3$ with $n = 9, 12, 15, 18, \ldots$ for the particular case where tridirectional growth is followed by termination at each step.

Polymerization Rate. The rate of step polymerization is the sum of the rates of reaction between molecules of various sizes in the propagation step, and it can be conveniently expressed in terms of the concentrations of the reacting functional groups,[26,31] in our case −OH and $-Al(CH_3)_2$. Using the concept of equal reactivity of functional groups,[26] the rate of polymerization can then be expressed as the rate of disappearance of the hydroxyl groups. At each propagation step, two such functional groups are consumed and the polymerization rate is given by

$$R_p = -\frac{d[-OH]}{dt} = k_p[-OH]^2 \quad (14)$$

Letting [Y] be the concentration of −OH functional groups at time t, the integration of the eq 14 yields

$$\frac{1}{[Y]} - \frac{1}{[Y]_0} = k_p t \quad (15)$$

where $[Y]_0$ is the initial (at $t = 0$) concentration of −OH functional groups and k_p is the rate constant for the propagation step, as stated previously. In terms of the extent or fraction of reaction, p, the concentration at time t is given by

$$[Y] = [Y]_0(1 - p) \quad (16)$$

The number-average degree of polymerization, $\bar{X}_n$, defined as the average number of structural units per polymer chain, is related to the extent of reaction by Carothers's equation,[32] which combined with eqs 15 and 16 yields

$$\bar{X}_n = \frac{1}{1 - p} \quad (17)$$

$$\frac{1}{1 - p} = \bar{X}_n = [Y]_0 k_p t + 1 \quad (18)$$

Considering the first-order kinetic dependence for the MAO formation, eq 18, a linear increase of the polymerization degree with time is expected, which is a characteristic of step polymerization. In fact, the available experimental data for step polymerization processes exhibit deviations from linearity, presenting an increased effect in the low conversion region and opposite effect in the high conversion region.[26]

C. MAO Chemical Composition. MAO composition is often characterized by the methyl-to-aluminum ratio, and the oxygen content is determined from the valence balance. The most commonly reported CH_3/Al ratio is in the range of 1.4−1.5;[1,27] values higher than 1.5 and lower than 1.4 have also been reported[7] and most importantly the ratio is always greater than 1. As seen in Table 2, the chemical composition of the structures that emerged from the proposed mechanism, the above cases (i), (ii), and (iii), is in the range of the experimental MAO chemical composition, with the CH_3/Al ratio always higher than 1, in contrast to the large majority of the previously proposed models[2] in which the ratio is equal to 1.

D. MAO Molecular Weight. The number-average molecular weight $\bar{M}_n$, defined as the total weight of a polymer sample divided by the total number of moles,[26] is given by

$$\bar{M}_n = M_0\bar{X}_n + n_t M_t \quad (19)$$

where M_0 is the mass of the monomer unit, n_t is the number of the terminal groups, and M_t is the molecular weight of the terminal groups, TMA in our case. Commonly, an average degree of polymerization of about 16 is reported[18] for MAO. Using eq 18, the number-average molecular weight is 1072 g/mol for the bidirectional growth (i), 1144 g/mol for the tridirectional growth (ii), and 1360 g/mol for the special case of the tridirectional growth (iii). Assuming an equal probability for these species, the average molecular weight is 1192 g/mol, which is in very good agreement with experiment, considering that the most commonly reported average molecular weight for MAO is 1200 g/mol.[7,29]

Table 2. CH_3:Al:O Ratio in the MAO Structures That Emerged from the Proposed Mechanism for Comparison with the Experimental Value for MAO, 1.3−1.5:1:0.7−0.8[1,7,27a]

n	(i)	(ii)	(iii)
8	1.40:1:0.80		
9		1.50:1:0.75	1.50:1:0.75
10	1.30:1:0.83		
12	1.29:1:0.86	1.40:1:0.80	1.60:1:0.67
14	1.25:1:0.87		
15		1.33:1:0.83	1.75:1:0.63
16	1.22:1:0.88		
18	1.20:1:0.90	1.29:1:0.86	1.80:1:0.60
20	1.18:1:0.91		
21		1.25:1:0.87	1.88:1:0.58
22	1.15:1:0.92		

[a] (i) Corresponds to bidirectional growth, whereas (ii) and (iii) correspond to tridirectional growth.

Conclusions

Initial steps in the formation of MAO by TMA hydrolysis have been studied using a combination of ab initio molecular dynamics and standard ab initio methods. A bifunctional monomer, $TMA-OH_2$, is formed by reaction of water and TMA_2. This monomer could further react to form a dimeric hydroxide ($M_2^{2''}$). For all the structures proposed herein, the presence of the dimeric hydroxide, the monomer, and TMA is enough to explain MAO formation though the proposed mechanism, which has all the characteristics of a step polymerization. All isolated *tert*-butylaluminoxane species are analogues of molecules predicted by the proposed mechanism. The dimeric hydroxide has been isolated after formation of $[(^tBu)Al(\mu_3\text{-}O)]_6$, $[(^tBu)Al(\mu_3\text{-}O)]_9$, and $[(^tBu)Al(\mu_3\text{-}O)]_{12}$ in large scale experiments.[6] This, along with the fact that for most step polymerizations there is less than 1% of the original monomer remaining at a point where the average polymer chain contains ∼10 monomer units, support the proposed mechanism. The dynamics of the reactant system presented in Figure 5 reveals an interesting insight: that the methyl bridges can be replaced by −OH groups. Ystenes, et al.[4] speculated about the replacement of MAO methyl bridges by −OH groups from water. After the formation of the hexameric cage, several reaction channels have been identified: a bidirectional growth generating rodlike structures as in M_8^7-11, a tridirectional growth as in M_8^7-13, a special case of tridirectional growth where each growth step is followed by a termination and methyl bridges are formed as in M_8^7-12, and several different structures from $M_7^{7'}-3$. The structures that emerged from the proposed mechanism are in agreement with crystallographic evidence for *tert*-butylalumi-

(32) Carothers, W. H. *Trans. Faraday Soc.* **1936**, *32*, 39.

noxanes, support the experimental data regarding MAO chemical composition, and contain the structural motif of bridging methyl groups thought to be essential for MAO cocatalytic activity,[4] which is a significant improvement over previously proposed models of MAO.

Acknowledgment. This study was supported by National Science Foundation grants CHE-0517236 and CHE-9977124. Calculations were performed on computers located at LSU's Center for Computation and Technology (www.cct.lsu.edu). We thank Dr. Jan L. Eilertsen for many useful conversations, both in person and through email, in particular about the evidence and nature of the bridging methyl motif.

Supporting Information Available: Coordinates of the optimized geometries for the presented structures, along with their energies, coordinates of the optimized geometries corresponding to the transition states in the calculated reaction paths, along with their energies, natural bond analysis, and the bonding orbital for the Al−O bond in $TMA-OH_2$, as well as complete refs 14 and 15. This material is available free of charge via the Internet at http://pubs.acs.org.

JA064545Q